LETTERS
PUBLISHED ONLINE: 3 APRIL 2017 | DOI: 10.1038/NMAT4888
nature materials

Surface-dominated conduction up to 240 K in the Kondo insulator SmB_6 under strain

A. Stern[1], M. Dzero[2], V. M. Galitski[3], Z. Fisk[1] and J. Xia[1]*

SmB_6 is a strongly correlated mixed-valence Kondo insulator[1,2] with a newly discovered surface state[3,4], proposed to be of non-trivial topological origin[5,6]. However, the surface state dominates electrical conduction only below $T^* \approx 4$ K (ref. 3), limiting its scientific investigation and device application. Here, we report the enhancement of T^* in SmB_6 under the application of tensile strain. With 0.7% tensile strain we report surface-dominated conduction at up to a temperature of 240 K, persisting even after the strain has been removed. This can be explained in the framework of strain-tuned temporal and spatial fluctuations of *f*-electron configurations, which might be generally applied to other mixed-valence materials. We note that this amount of strain can be induced in epitaxial SmB_6 films via substrate in potential device applications.

SmB_6 is a prototypical Kondo insulator, a material where the quantum mechanical hybridization between the conduction and *f*-electronic orbitals leads to an opening of a narrow Kondo gap near the Fermi energy[1,2]. Experimental observations of the robust surface conductivity on the background of the fully insulating bulk[3,4] and quantum oscillations from a two-dimensional surface[7] both contribute to the highly non-trivial nature of an insulating state in SmB_6. SmB_6 has so far attracted much attention as a prominent candidate material for a strongly correlated topological insulator[5,6,8]. It is noteworthy to mention that the first application of SmB_6 as a radiofrequency micro-oscillator device[9] has been recently demonstrated, operating at cryogenic temperatures.

Due to the small value of the bandgap Δ, scientific investigations and device applications of SmB_6 have thus far been limited to temperatures below the resistance saturation temperature $T^* \approx 4$ K when the surface conduction becomes larger than the bulk conduction[3,4], motivating the search for means of enhancing T^*. In the context of thin films, it is known that strain induced by a substrate can dramatically change the temperature scale of the physical phenomena, such as the room-temperature ferroelectricity in strained $BaTiO_3$ (ref. 10). In SmB_6, it has been shown that Δ can be reduced and eventually quenched[11] with an external pressure of up to 50 kbar. Consequently, T^* decreases to zero under pressure[11,12]. A comprehensive theoretical explanation of this intriguing phenomenon has not been reported yet, although it has been speculated to be related to the pressure-dependent valence of Sm ions[11]. A related question of whether negative pressure (tensile strain) would alter Δ or T^* in SmB_6 has also not been addressed yet.

Applying a large amount of tensile strain in a controllable fashion to macroscopic crystals has been difficult until very recently when a tri-piezo technique[13] was introduced to enhance the superconducting transition temperature of Sr_2RuO_4 with strain, which is the fractional change of the sample length[14]. For this study we have adopted this technique and constructed a strain set-up that can apply between −0.5% and 1% strain to SmB_6 crystals (see Methods). As shown in Fig. 1a, the piezo stacks and titanium pieces are arranged so that they compensate for differential thermal contraction[13]. Naturally needle-shaped SmB_6 crystals obtained directly from growth were mounted to the gap between the titanium pieces using hard cryogenic epoxy. Strain gauges were used to measure the length change of the piezos, which was used in turn to estimate the strain in SmB_6 using calibration with direct cryogenics microscopic imaging. At $T = 4$ K, we found that more than 70% of the strain is transferred from the piezos to the SmB_6 needle crystals (see Supplementary Information for details), which is comparable to what has been seen in Sr_2RuO_4 (ref. 14). With a cubic symmetry and a Poisson's ratio of $\eta = -0.0213$ (ref. 15), all dimensions of SmB_6 expand with tensile strain, making it quite analogous to negative hydrostatic pressure.

In Kondo insulators the value of an insulating gap is usually obtained by fitting the bulk-dominated conduction region to $R^{-1}/R_{\mathrm{bulk}}^{-1} = \exp(-\Delta/k_{\mathrm{B}}T)$ (ref. 11), where R_{bulk} is a resistance constant for the bulk, T is the temperature, R is the measured resistance, and Δ is the bandgap. As shown in Fig. 1b for a $\langle 100 \rangle$-oriented SmB_6 crystal, when a small compressive strain ($-0.4\% \leq \epsilon < 0$) is applied, we found that Δ is reduced by as much as 30%, comparable to an applied pressure of 24 kbar (ref. 11). Given a low-temperature bulk modulus of 910 kbar (ref. 16) for SmB_6, $\epsilon = -0.4\%$ strain is roughly equivalent to 24 kbar, which again agrees with high-pressure results[11].

In contrast, as we show in Fig. 1c, a small tensile strain results in exactly the opposite behaviour: the resistance saturation temperature T^* is shifted to higher temperatures and Δ is enhanced by 50%, suggesting that it has a similar origin to the yet unknown mechanism for pressure-induced Δ reduction[11]. We note that changes in the values of Δ are much sharper when $|\epsilon| \geq 0.4\%$, suggesting a well-defined collective response for both negative and positive strain.

While compressive strain beyond $\epsilon = -0.5\%$ tends to break needle-shaped samples probably due to shear strain, much larger tensile strains can be safely applied. Shown in Fig. 2a for another $\langle 100 \rangle$-oriented SmB_6 crystal, sample B, tensile strains up to 0.66% continuously increase the resistance saturation temperature T^* up to 30 K. We note that in this sample in contrast with sample A, the surface-dominated saturation resistance is strongly dependent on applied strain, reminding us of the similarly diverse behaviours observed in high-pressure experiments[11,12,17,18] (see Supplementary Information). Surprisingly, when $\epsilon \geq 0.7\%$ we observe a dramatic onset of hysteretic behaviour in the resistivity of SmB_6. Note that the possibility of piezo hysteresis can be ruled out by careful experimental analysis (see Supplementary Information on

[1]Department of Physics and Astronomy, University of California, Irvine, California 92697, USA. [2]Department of Physics, Kent State University, Kent, Ohio 44242, USA. [3]Joint Quantum Institute, Department of Physics, University of Maryland, College Park, Maryland 20742, USA.
*e-mail: xia.jing@uci.edu

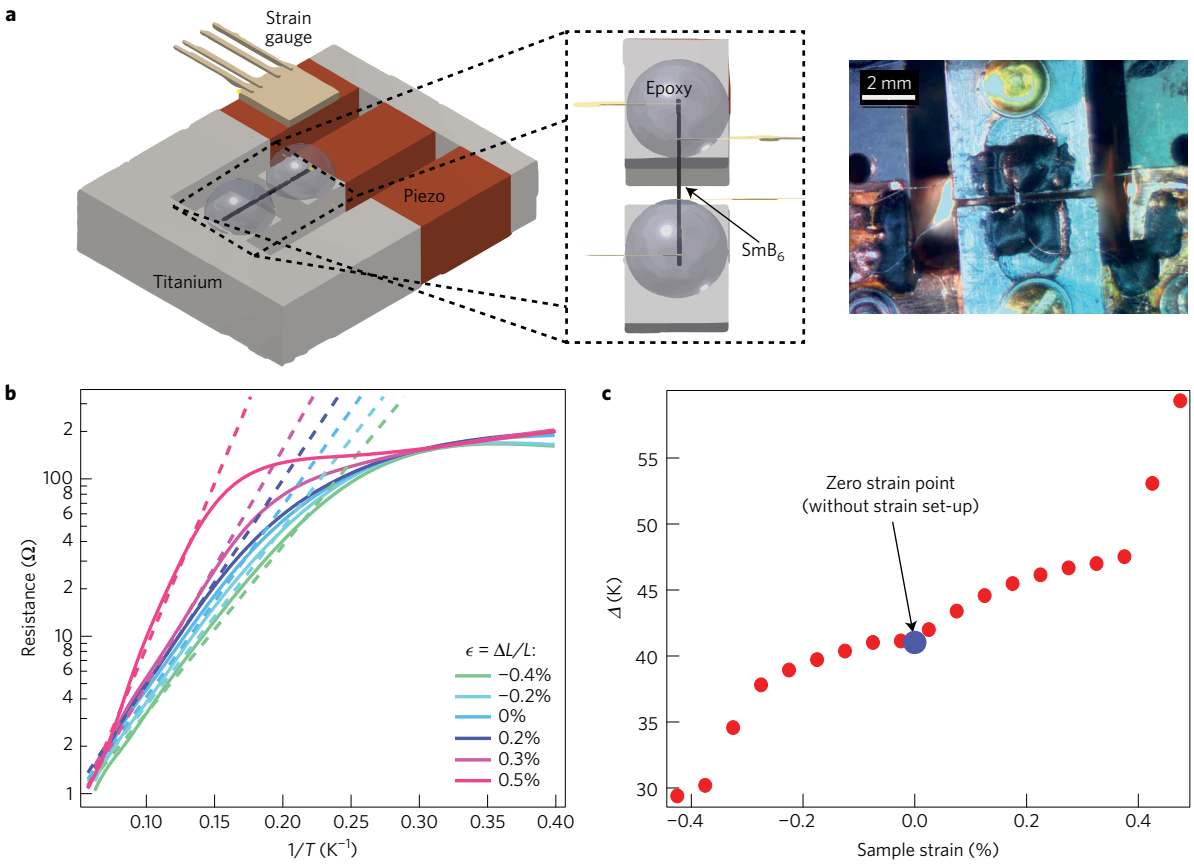

Figure 1 | Experimental set-up and gap enhancement with tensile strain in sample A. a, Sketch and photo of the strain apparatus with a SmB_6 sample (more details in Supplementary Information). **b**, The resistance of a (100)-oriented crystal as a function of inverse temperature when subject to a relatively small strain between −0.4% and 0.5%. The dashed lines are linear fits. The extracted bandgap Δ is measured from the slope of the curve (dashed line) in the bulk-dominated conduction region. **c**, The extracted bandgap, which increases with tensile strain and decreases with compressive strain. The blue dot is the Δ of the strain-free state before the sample is mounted to the stain set-up.

discussion of this issue). As shown in Fig. 2b with sample A, at an elevated temperature of 30 K and at tensile strains $\epsilon \geq 0.7\%$ the resistance increases suddenly by more than two orders of magnitude from the bulk-dominated resistance of 1 Ω to the surface-dominated resistance of ∼100 Ω, indicative of a first-order phase transition. This dramatic phenomenon is hysteretic in nature: when the strain is reduced to 0% the sample resistance maintains its surface-dominated value until a compressive strain is applied. However, after an application of a large tensile strain, the bulk of SmB_6 remains insulating with a significantly increased temperature T^* even after the strain is removed.

To measure the upper bound of T^*—the temperature below which the surface conduction is dominant—we prepared sample C. This sample has been strained at low temperature with $\epsilon = 0.9\%$, the strain was reduced back to zero and the sample was warmed up to 300 K. It is shown in Fig. 2c, where the blue curve represents the initial cool down without strain and the red curve shows the warm up after the tensile strain has been applied at low temperature. The noise in the resistance value at temperatures between 40 K and 240 K is quite repeatable between measurements, suggestive of an underlying fluctuations in the system, which will be discussed below. The sample resistance remains to be more than three orders of magnitude larger than the bulk-dominated value (blue curve) normally observed at these temperatures until the temperature reaches $T^* = 240$ K when it suddenly reverts back to the bulk resistance value of 0.07 Ω. To our knowledge, this T^* is over double the observed value in topological insulator films of Bi_2Se_3 (ref. 19) and Bi_2Te_3Se (ref. 20).

Up to this point we have presented experimental observation of two effects: surface-dominated transport in SmB_6 at temperatures above 200 K and hysteresis in resistivity under an application of tensile strain. To provide the qualitative understanding of the observed phenomena, we recall that it has been well established experimentally[21,22] that SmB_6 belongs to a class of intermediate valence systems: the f-orbital electronic configuration of samarium ions fluctuates between the $4f^5$ and $4f^6$ states on a typical timescale τ_{ivc} across a fairly wide temperature range. Experiments that probe the samarium valence on a timescale longer than τ_{ivc} will observe an intermediate valence state[23,24]. Experimentally found values of an intermediate valence configuration vary slightly between $Sm^{2.5+}$ and $Sm^{2.6+}$, suggesting that the energies for the corresponding integer valence configurations are comparable to each other, $E(f^5) \sim E(f^6)$.

With a decrease in temperature, emerging hybridization between the d-orbital and f-orbital states of samarium opens up a scattering channel $4f^6 \leftrightarrow 4f^5 + 5d$ leading to an onset of insulating behaviour at low temperatures and also to small changes in the intermediate valence configuration[21]. Since the ionic volume corresponding to the $4f^6$ configuration exceeds the one for the $4f^5$ configuration, the energy difference between the corresponding valence configurations $\Delta E = E(f^6) - E(f^5)$ will increase with pressure and the scattering processes $4f^6 \leftrightarrow 4f^5 + 5d$ will be suppressed. As a consequence, one expects that the material recovers its metallic properties in the bulk. On the other hand, an application of a tensile strain acts as a negative pressure and therefore should have an opposite effect of enhancing the insulating behaviour and promoting stronger hybridization between the d- and f-orbitals.

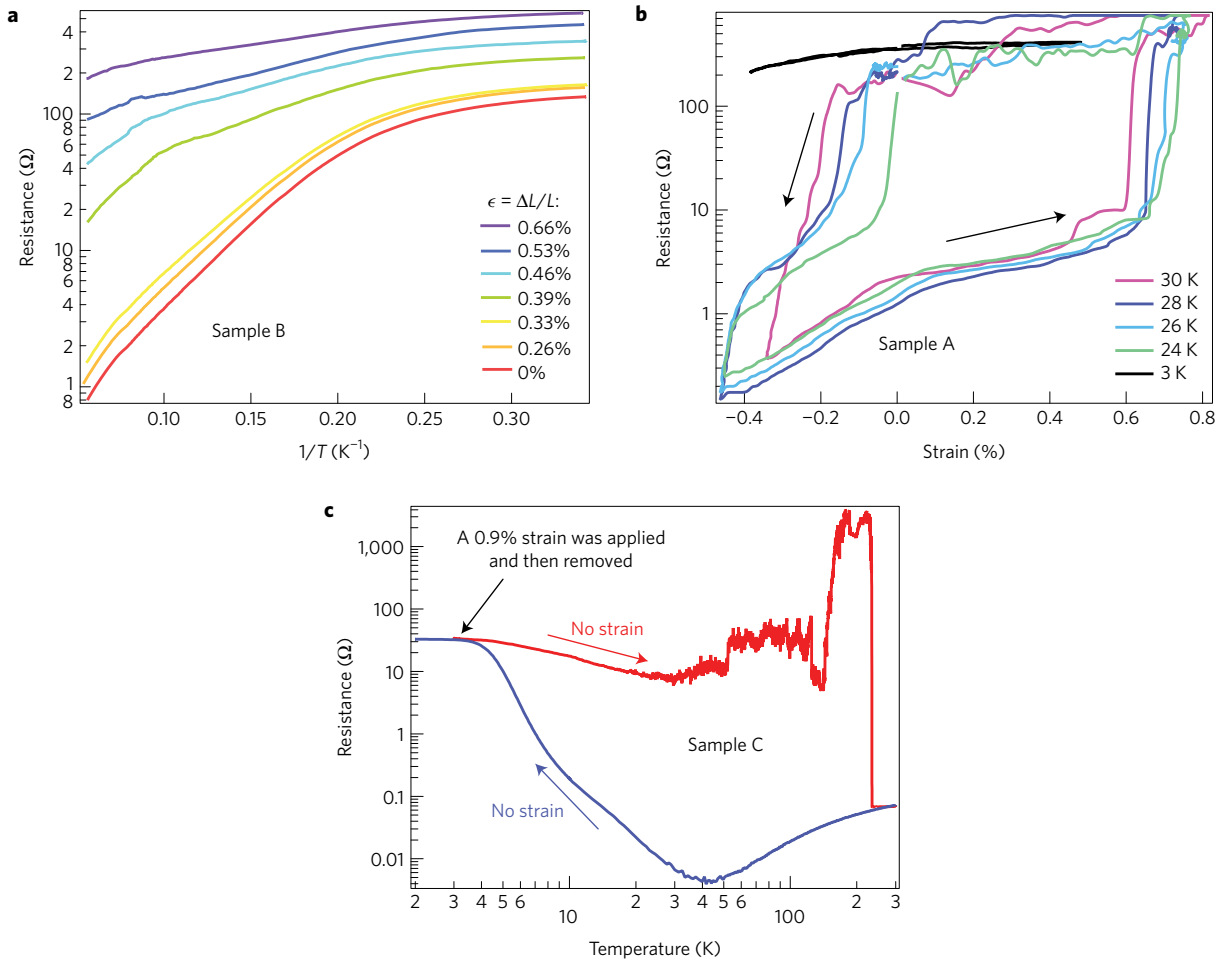

Figure 2 | Hysteresis and room-temperature surface-dominated conduction. a, The enhancement of T^* with tensile strain $\epsilon \leq 0.66\%$ in sample B. Unlike sample A the low-temperature saturation (surface) resistance in this sample is strain dependent, similar to what was found under pressure in ref. 11. **b**, The occurrence of hysteresis with $\epsilon \geq 0.6\%$ in sample A. Data shown here represent measurements after the sample has been strained beyond 0.7%. **c**, The persistence of surface-dominated conduction up to 240 K, after a strain of $\epsilon = 0.9\%$ was applied and then removed at low temperature in sample C.

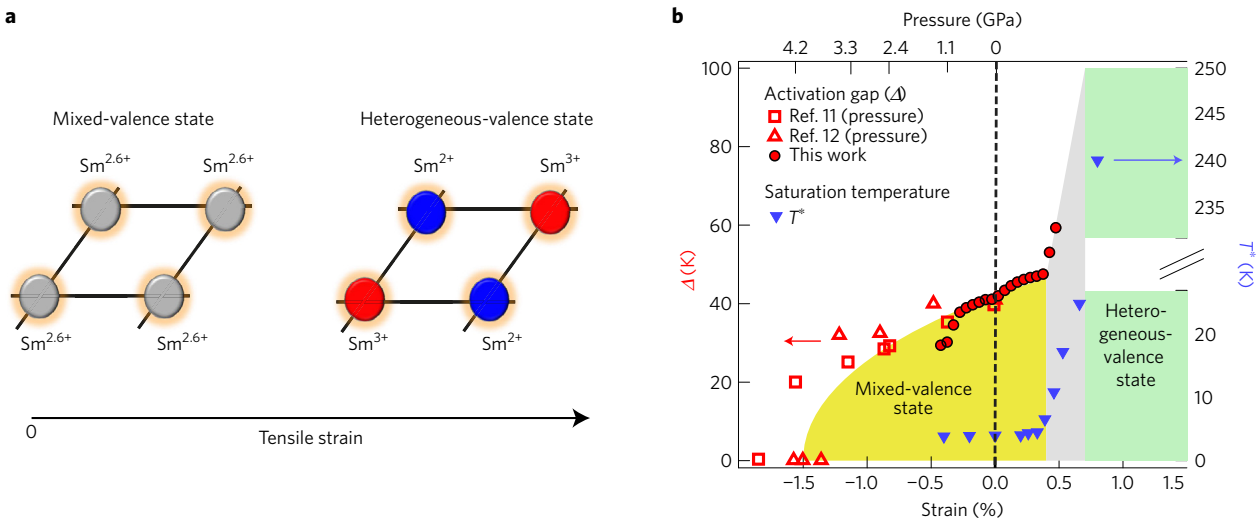

Figure 3 | Temperature–strain phase diagram. a, A schematic illustration of strain-induced transition from temporal fluctuating mixed-valence state to spatially heterogeneous-valence state. **b**, A reconstructed phase diagram of SmB_6 under strain with data from this paper as well as pressure data from refs 11,12. The left axis corresponds to the bandgap data in ref. 12 (open red triangles), the bandgap data in ref. 11 (open red squares), and our own bandgap data (red circles). The right axis corresponds to only T^*, which is shown in blue downtriangles.

Our experimental results for the small tensile strain confirm these expectations.

While an increase in T^* with tensile strain can be qualitatively understood by the argument based on the changes in the ionic volume, our observation of hysteresis in resistivity as a function of temperature points towards the emergence of the spatial inhomogeneities. Since the energies of the Sm^{2+} and Sm^{3+} become almost degenerate the characteristic timescale τ_{ivc} will increase. Ultimately, $\tau_{ivc} \rightarrow \infty$ and the system is expected to develop spatially inhomogeneities by becoming mixed-valent: each samarium ion will be in either the Sm^{2+} or Sm^{3+} integer valence state, as we have schematically shown in Fig. 3a. Accordingly we constructed a phase diagram shown in Fig. 3b: it illustrates the change from mixed- to heterogeneous-valence state, in comparison with high-pressure experiments[11,12]. Note, however, as was discussed in ref. 23, transition into the spatially inhomogeneous state would be energetically costly since it would mean the departure from the simple rock salt crystal structure. However, in our experiments the energy costs are offset by a tensile strain. Finally, we note that an abrupt jump in the value of T^* signals the first-order transition; however, its value is most probably affected by the local strain and Coulomb interactions between electrons in the Sm^{2+} and Sm^{3+} valence states, so that this change in T^* may not reflect the corresponding changes in the bulk hybridization gap.

Most recently, SmB_6 has been discussed as a prominent candidate for the first correlated topological insulator. One of the major experimental issues with identifying the topological nature of the metallic surface states has been the smallness of the insulating gap precluding, for example, the precise measurement of the surface electron's chirality. Our experimental findings show that this issue can be, in principle, resolved. On a more general note, our results confirm the basic idea that topological Kondo insulators are likely to be found in systems in the intermediate valence rather than local moment regime.

Methods

Methods, including statements of data availability and any associated accession codes and references, are available in the online version of this paper.

Received 16 September 2016; accepted 6 March 2017; published online 3 April 2017

References

1. Fisk, Z. *et al*. Kondo insulators. *Physica B* **223,** 409–412 (1996).
2. Riseborough, P. S. Heavy fermion semiconductors. *Adv. Phys.* **49,** 257–320 (2000).
3. Kim, D. J. *et al*. Surface Hall effect and nonlocal transport in SmB_6: evidence for surface conduction. *Sci. Rep.* **3,** 3150 (2013).
4. Wolgast, S. *et al*. Low-temperature surface conduction in the Kondo insulator SmB_6. *Phys. Rev. B* **88,** 180405 (2013).
5. Dzero, M., Sun, K., Coleman, P. & Galitski, V. Theory of topological Kondo insulators. *Phys. Rev. B* **85,** 045130 (2012).
6. Alexandrov, V., Dzero, M. & Coleman, P. Cubic topological Kondo insulators. *Phys. Rev. Lett.* **111,** 226403 (2013).
7. Li, G. *et al*. Two-dimensional Fermi surfaces in Kondo insulator SmB_6. *Science* **346,** 1208–1212 (2014).
8. Dzero, M., Sun, K., Galitski, V. & Coleman, P. Topological Kondo insulators. *Phys. Rev. Lett.* **104,** 106408 (2010).
9. Stern, A., Efimkin, D. K., Galitski, V., Fisk, Z. & Xia, J. Radio frequency tunable oscillator device based on a SmB_6 microcrystal. *Phys. Rev. Lett.* **116,** 166603 (2016).
10. Choi, K. *et al*. Enhancement of ferroelectricity in strained $BaTiO_3$ thin films. *Science* **306,** 1005–1009 (2004).
11. Cooley, J. C., Aronson, M. C., Fisk, Z. & Canfield, P. C. SmB_6: Kondo insulator or exotic metal? *Phys. Rev. Lett.* **74,** 1629–1632 (1995).
12. Derr, J. *et al*. From unconventional insulating behavior towards conventional magnetism in the intermediate-valence compound SmB_6. *Phys. Rev. B* **77,** 193107 (2008).
13. Hicks, C. W., Barber, M. E., Edkins, S. D., Brodsky, D. O. & Mackenzie, A. P. Piezoelectric-based apparatus for strain tuning. *Rev. Sci. Instrum.* **85,** 065003 (2014).
14. Hicks, C. W. *et al*. Strong increase of T_c of Sr_2RuO_4 under both tensile and compressive strain. *Science* **344,** 283–285 (2014).
15. Goldstein, R. V., Gorodtsov, V. A. & Lisovenko, D. S. Relation of Poisson's ratio on average with Young's modulus. Auxetics on average. *Dokl. Phys.* **57,** 174–178 (2012).
16. Tamaki, T. *et al*. Elastic properties of SmB_6 and Sm_3Se_4. *J. Magn. Magn. Mater.* **47,** 469–471 (1985).
17. Beille, J., Maple, M. B., Wittig, J., Fisk, Z. & DeLong, L. E. Suppression of the energy gap in SmB_6 under pressure. *Phys. Rev. B* **28,** 7397–7400 (1983).
18. Moshchalkov, V. V. *et al*. SmB_6 at high pressures: the transition from insulating to the metallic Kondo lattice. *J. Magn. Magn. Mater.* **47,** 289–291 (1985).
19. Ren, Z., Taskin, A. A., Sasaki, S., Segawa, K. & Ando, Y. Large bulk resistivity and surface quantum oscillations in the topological insulator Bi_2Te_2Se. *Phys. Rev. B* **82,** 241306 (2010).
20. He, L. *et al*. Surface-dominated conduction in a 6 nm thick Bi_2Se_3 thin film. *Nano Lett.* **12,** 1486–1490 (2012).
21. Mizumaki, M., Tsutsui, S. & Iga, F. Temperature dependence of Sm valence in SmB_6 studied by X-ray absorption spectroscopy. *J. Phys. Conf. Ser.* **176,** 012034 (2009).
22. Butch, N. P. *et al*. Pressure-resistant intermediate valence in the Kondo insulator SmB_6. *Phys. Rev. Lett.* **116,** 156401 (2016).
23. Varma, C. M. Mixed-valence compounds. *Rev. Mod. Phys.* **48,** 219–238 (1976).
24. Lawrence, J. M., Riseborough, P. S. & Parks, R. D. Valence fluctuation phenomena. *Rep. Prog. Phys.* **44,** 1–84 (1981).

Acknowledgements

This work was supported by NSF grant DMR-1350122. V.M.G. acknowledges the support from DOEBES (DESC0001911) and Simons Foundation. M.D. acknowledges the support from NSF (DMR-1506547). We thank S. Thomas, B. Casas and D. Trinh for technical assistance.

Author contributions

A.S. performed the measurements. M.D. and V.M.G. developed the theory. Z.F. fabricated the samples. J.X. designed the project. All authors discussed the result, and contributed to the writing of the manuscript.

Additional information

Supplementary information is available in the online version of the paper. Reprints and permissions information is available online at www.nature.com/reprints. Publisher's note: Springer Nature remains neutral with regard to jurisdictional claims in published maps and institutional affiliations. Correspondence and requests for materials should be addressed to J.X.

Competing financial interests

The authors declare no competing financial interests.

Methods

Single-crystal growth. All samples were grown by the aluminium flux method and HCl was used to remove any aluminium flux or impurities on the samples. Samples were selected on the basis of their dimensions, which was possible due to the abundance of SmB_6 samples at our disposal. Samples were then polished to remove any surface cracks, which can cause the samples to break prematurely.

Strain apparatus. The strain apparatus is composed of titanium and piezo stacks to limit the effects of thermal contraction/expansion shown in Supplementary Information, Fig. 1. All of the piezo movement is applied to a narrow gap where the sample is mounted using Stycast 2850FT epoxy with catalyst 24 LV. Strain gauges were mounted on the piezo stacks and calibrated using an optical microscope at low temperatures.

Transport measurement. We measured resistance using a Signal Recovery 7225 DSP lock-in amplifier. The corresponding gap Δ is obtained by fitting the bulk-dominated conduction region to $R = R_{\mathrm{bulk}} \exp(\Delta / k_{\mathrm{B}} T)$, where, R_{bulk} is a resistance constant for the bulk, T is the temperature, R is the measured resistance, and Δ is the bandgap.

Data availability. The data that support the findings of this study are available from the corresponding author on reasonable request.